PAPER

Check for updates

Experimental study of CO_2 capture by nanoparticle-enhanced 2-amino-2-methyl-1-propanol aqueous solution

Qiuli Zhang, [ID] *[a] Zhongyi Ning,[a] Xuelian Li,[a] Xiaogang Ning,[b] Fan Wu [ID] [b] and Jun Zhou[a]

2-Amino-2-methyl-1-propanol (AMP) is often used as a moderator to enhance the CO_2 capture capacity of absorbents due to its unique spatial site resistance structure, and relatively few studies have been conducted on the enhancement of AMP aqueous solutions by nanoparticles for CO_2 capture. In order to investigate the effect of nanoparticles on the CO_2 capture performance of AMP aqueous solution, different nanofluids were formulated in this paper using a two-step method, and a bubbling reactor and an oil bath were used as the experimental setup for absorption/desorption, and through comparative experiments, it was found that the type of nanoparticles, the solid content, and the different parameters have great influences on the CO_2 absorption load and desorption rate. The experimental results show that the addition of TiO_2 nanoparticles to the AMP base solution can accelerate the absorption–desorption mass transfer rate of CO_2, and there exists an optimal solid content of 1 g L^{-1} (±1.0%, ±2.5%); after multiple absorption–desorption experiments, good cycling performance can still be achieved. The experimental results of the nanofluid-promoted mass transfer mechanism are also illustrated and analyzed in this paper.

1 Introduction

CO_2 has become the most major greenhouse gas with the amount of CO_2 in the atmosphere increasing by about 25% since the industrial revolution.[1] In particular, the burning of fossil fuels such as oil and coal in industrial production accumulates large quantities of CO_2 and other gases, and these greenhouse gases not only cause a series of ecological and environmental problems, but also result in huge economic losses. Nowadays, scientific and technological developments have made it possible to capture, utilize and store CO_2 from industrial exhaust gases or directly from the air.[2,3] Monoethanolamine (MEA) is usually the most widely used chemical absorbent for industrial applications, but its regeneration energy consumption is as high as 3.2–4.0 GJ ton$^{-1}CO_2$, and such a high renewable energy consumption increases the cost of CO_2 capture, so there are obvious limitations for large-scale commercial applications.[3,4] Space-site-resistant amines are often used as modulators and are characterized by bulky groups adjacent to the amino group. Due to the influence of space-site resistance, they are prone to form unstable carbamates when reacting with CO_2 and decompose easily in carbonates,[5] and

currently widely studied is 2-amino-2-methyl-1-propanol (AMP). Wai *et al.*[6] showed that AMP aqueous solutions have a high capacity for CO_2 absorption, good thermal stability, and the existence of the site resistance effect makes AMP highly degradable and have low regeneration energy. Han *et al.*[7] compared the CO_2 absorption capacity of AMP with MEA and found that the absorption rate of AMP was slightly lower than MEA. In addition, many studies have been reported on the physicochemical and thermodynamic properties of AMP such as corrosion rate, density, viscosity and regeneration performance in mixed amine solvents.[8,9]

Recently, research on the use of nanofluids to enhance mass transfer and reduce energy consumption has been actively underway. According to previous studies, it has been found that nanoparticles have a high specific surface area, and when small amounts are introduced into the base solution of organic amine absorbents by physical or chemical methods,[10,11] absorbents are acquired with enhanced CO_2 absorption performance and other advantages (*e.g.*, improved solvent stability and reduced solvent vapor pressure, *etc.*).[12] Meanwhile, nanoparticles can reduce the mass transfer resistance of gas–liquid two-phase and accelerate the mass transfer rate, thereby reducing energy consumption.[13,14] TiO_2 is a nanoparticle with high CO_2 adsorption capacity, which was found to be due to the presence of oxygen vacancies in TiO_2 nanoparticles, which introduce additional adsorption sites.[22,37] Fang *et al.*[49] researched the effect of nanoparticles on CO_2 absorption in ammonia and found that

[a]*School of Chemistry and Chemical Engineering, Xi'an University of Architecture and Technology, Xi'an, Shaanxi 710055, China. E-mail: qiulizhang@126.com*

[b]*Shaanxi Beiyuan Chemical Industry Group Co., Ltd, Jinjie Industrial Park, Shenmu 719319, China*

TiO_2 nanoparticles can enhance the gas–liquid mass transfer process of chemical reactions. Kim et al.[15] conducted CO_2 absorption experiments through utilizing SiO_2 nanoparticles in a bubbling absorber of a water-based nanofluid. It was demonstrated that the addition of nanoparticles increased the total absorption rate by 24%. Lee et al.[16] and Ma et al.[17] employed Al_2O_3, carbon nanotubes (CNTs) and other nanoparticles to study the CO_2 absorption process in NH_3/H_2O solution. Moreover, Kim et al.[18] measured the vapor absorption rate of a falling film type $H_2O/LiBr$ for CO_2 absorption process employing SiO_2 nanoparticles and reported a maximum enhancement of mass transfer rate up to 18%. While there are many studies on enhanced CO_2 absorption,[15–21] considering the advantages of AMP in solvent utilization, further studies on the unique and superior properties of nanofluids when AMP is used as a base fluid, which have not yet been reported, are needed for further development of AMP absorption systems. In this work, AMP-based nanofluids were utilized to control the CO_2 capturing performance in order to enhance the absorption and desorption rate, as well as to improve its recycling performance.

Herein, we have systematically investigated the effects of type, concentration and different parameters of nanofluid on the absorption–desorption of CO_2 based on 2-amino-2-methyl-1-propanol (AMP), and proposed the mechanism of the enhanced CO_2 absorption and regeneration performance of AMP-based nanofluid. The experimental results provide a theoretical basis for the development of new hybrid absorbents with high absorption capacity, fast absorption rate and good desorption performance.

2 Experiment

2.1 Experimental materials and instruments

Herein, the following reagents were used: 2-amino-2-methyl-1-propanol (AMP), Shanghai McLean Biochemical Science and Technology Co. Ltd; CO_2 gas with a purity (v/v) of 99.99%, Shaanxi Chang' an Gas Co. Ltd; TiO_2 (anatase, 99.7%, 15 nm), Al_2O_3 (α-phase, 99.6%,10–15 nm), SiO_2 (99.6%, 15 nm), Shanghai McLean Biochemical Science and Technology Co. Ltd; deionized water. The instruments used in this study are gas mass flow meter, electronic balance, ultrasonic crusher, water bath, oil bath, CO_2 gas analyzer, soap film flow meter.

During the experiments, the amount of CO_2 and the pressure inside the reactor were recorded continuously. Pressure measurements were performed using an Omega pressure sensor with an accuracy of ±1.0% and a temperature sensor with an accuracy of ±2.7 K (at 100 °C). And the uncertainty of CO_2 absorption was evaluated and determined to be ±2.1% for the pure solvent and ±1.0% for the nanofluidic absorbents. The uncertainty was ±2.0% for pure solvent desorption and ±2.5% for nanofluid determination.

2.2 Preparation of nanofluids

The different nanofluids were prepared by a two-step method before the experiment. Firstly, 15 wt% AMP aqueous solution was configured in advance as the absorbent base solution, then a certain amount ($0.2/0.5/1.0/1.5/2.0$ g L^{-1}) of nanoparticles was added to the base solution, followed by magnetic stirring for 30 min. Afterwards, the nanoparticles were dispersed by continuous cycling in an ultrasonic cleaner. In this study, different types of nanoparticles were used, including: TiO_2, Al_2O_3 and SiO_2. In order to avoid a rapid increase in the temperature of the solution, the experiment was carried out by intermittent vibration, with two seconds of vibration followed by two seconds of interval, and the effective vibration time was 60 min.

2.3 Experimental setup and procedure

The experimental system for nanoparticle-enhanced AMP solution absorption and desorption of CO_2 is shown in Fig. 1. The absorption process takes place in a bubbling reactor, where the gas output from the CO_2 cylinder is controlled and maintained at a certain pressure and mass flow rate via a gas mass flow meter. Pour 100 g of the pre-prepared nanofluid into the reactor, the water bath was heated to 40 °C ahead of time, and pure CO_2 gas with purity >> 99% was supplied to the bottom of the bubble absorber (3) at a given flow rate, and the counter-current flow was directed to the liquid absorbent supplied to the top of the absorber to produce absorption, and the CO_2 absorption was determined by the measurements of the mass of the solution at intervals of 10 min (g CO_2 per 100 g of the solution).

The desorption experiments were conducted in a three-necked flask with the rotor inserted and the flask corked tightly. The temperature of the oil bath was set to 120 °C in advance, and the three-necked flask was placed in it with magnetic stirring turned on, noting that the start of stirring was recorded as the reaction 0 moment. The temperature of the absorbent is increased by the heat exchange, which reduces the solubility of CO_2 and separates CO_2 from the absorbent. Impurities are similarly removed through the condenser tube so that only pure CO_2 is measured. The desorbed CO_2 was dried in a drying flask and entered into a soap film flowmeter, where the rate of desorption CO_2 (mL min^{-1}) at that moment was recorded. Measured flow rates were always corrected for the vapor pressure of water as a function of temperature. The initial solution volume is 100 mL, assuming that the solution volume does not change during the entire reaction.

2.4 Data analysis

In the absorption experiments, the CO_2 loading in the liquid phase (α, mol CO_2 per mol amine) was used to express the CO_2 absorption performance as shown in eqn (1). In these tests, in order to investigate the CO_2 desorption performance of the nanofluids, the desorption efficiency x is the ratio of the amount of substance of CO_2 desorbed to the amount of substance of CO_2 absorbed in total by the enriched fluid as shown in eqn (2).

It should be noted that the enhancement factor is usually defined as the ratio of the mass transfer coefficient of the nanofluid to the pure solution, and is used to evaluate the mass transfer enhancement of nanoparticles. In this work, the total CO_2 uptake (mol CO_2 per mol amine) was used to evaluate the
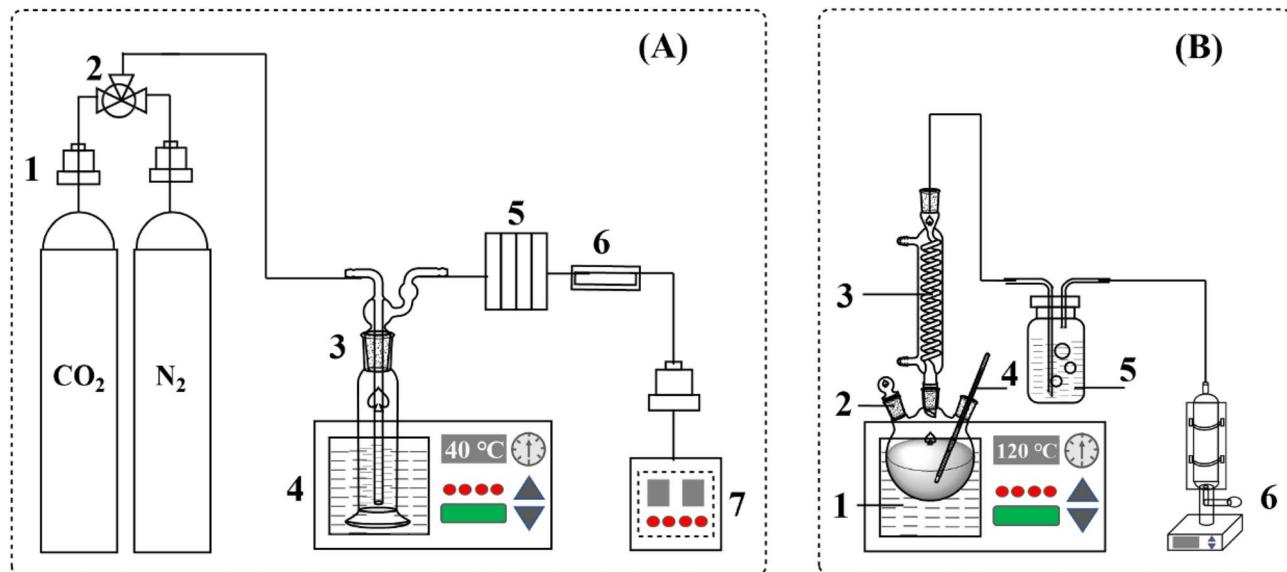
Fig. 1 (A) Bubble absorption reaction device: 1-mass flow meter; 2-tee valve; 3-bubble absorption tube; 4-water bath; 5-condensation tube; 6-drying tube (glass tube with color-changing silica gel); 7-CO_2 gas analyzer. (B) Desorption reaction device: 1-oil bath; 2-three-neck flask; 3-snake condenser tube; 4-laboratory thermometer; 5-drying flask (glass bottle with concentrated sulfuric acid); 6-soap film flow meter.

absorption performance of the absorbent. The enhancement factor is defined here as the ratio of the total amount of CO_2 absorbed/desorbed by the nanofluid to the pure AMP base fluid, denoted by E_{abs} and E_{des}, respectively, as shown in eqn (3) and (4), so that the effect of the nanoparticles on CO_2 absorption/desorption can be investigated. All experiments were repeated three times to avoid uncertainty in the experimental results.

$$\alpha = \frac{m/M_{CO_2}}{m_0/M_0} \quad (1)$$

$$x = \frac{n_{des(CO_2)}}{n_{abs(CO_2)}} \quad (2)$$

$$E_{abs} = \frac{n_{CO_2-nanofluid}}{n_{CO_2-pure\ solution}} \quad (3)$$

$$E_{des} = \frac{x_{(CO_2-nanofluid)}}{x_{0(CO_2-pure\ solution)}} \quad (4)$$

where m, m_0, M_{CO2}, M_0, $n_{des(CO_2)}$, and $n_{abs(CO_2)}$ are defined as the mass of CO_2 absorbed (g), the mass of amine in solution when no CO_2 is absorbed (g), the molar mass of CO_2 (g mol^{-1}), the molar mass of amine (g mol^{-1}), the amount of CO_2 desorbed in mol, and the amount of CO_2 absorbed in total by the enriched solution in mol, respectively.

3 Results and discussion

3.1 Absorption performance

3.1.1 Effect of nanofluid type. As can be seen from Fig. 2A, when the molar concentration of the AMP base solution is certain, the CO_2 absorption rate of several nanofluids is greater than that of the pure solution during the first 40 min of absorption. There is a gradual decrease in the rate of CO_2

uptake for each absorber as the reaction proceeds, due to the fact that the solution is saturated at this point.

The real-time absorption loading of all three nanofluids was also greater than that of the pure AMP solution at the initial stage (*i.e.*, within 10–40 min) (Fig. 2B), suggesting that the addition of nanoparticles can enhance the absorption loading of CO_2. Furthermore, the total CO_2 absorption of TiO_2-AMP nanofluid increased by 4.32% and Al_2O_3-AMP nanofluid increased by 3.71% than the pure AMP solution during 0–120 min, whereas the total CO_2 absorption of SiO_2-AMP nanofluid increased by only 1.39% than the pure AMP solution. This may be due to the fact that TiO_2 nanoparticles contain more oxygen vacancies and can adsorb more CO_2 molecules. Since the absorption of CO_2 is nearly saturated in the solution after 120 min, the absorption process only lasted for 120 min in the following tests.

3.1.2 Effect of nanoparticle solid content. In order to investigate the effects of different types of nanoparticles with different solid contents on CO_2 absorption mass transfer enhancement, three types of nanoparticles of the same size (15 nm) were used in this study. It was found that the CO_2 absorption enhancement factor of the nanofluids increased when the solid content of the nanoparticles was increased from 0.2 g L^{-1} to 1.0 g L^{-1}. However, after the solid content of nanoparticles reached 1 g L^{-1}, the absorption enhancement factor gradually decreased (Fig. 3). As can also be seen from the figure, the absorption enhancement factor of TiO_2-AMP nanofluid is better than other two nanofluids. The similar phenomenon was also reported by Turanov.[22] In other words, the optimum solid content of nanoparticles enhances the CO_2 absorption loading. Kesshishian *et al.*[23,24] also reported the presence of optimum solid content. As solid content increases, the number of nanoparticles in the mass transfer film increases,
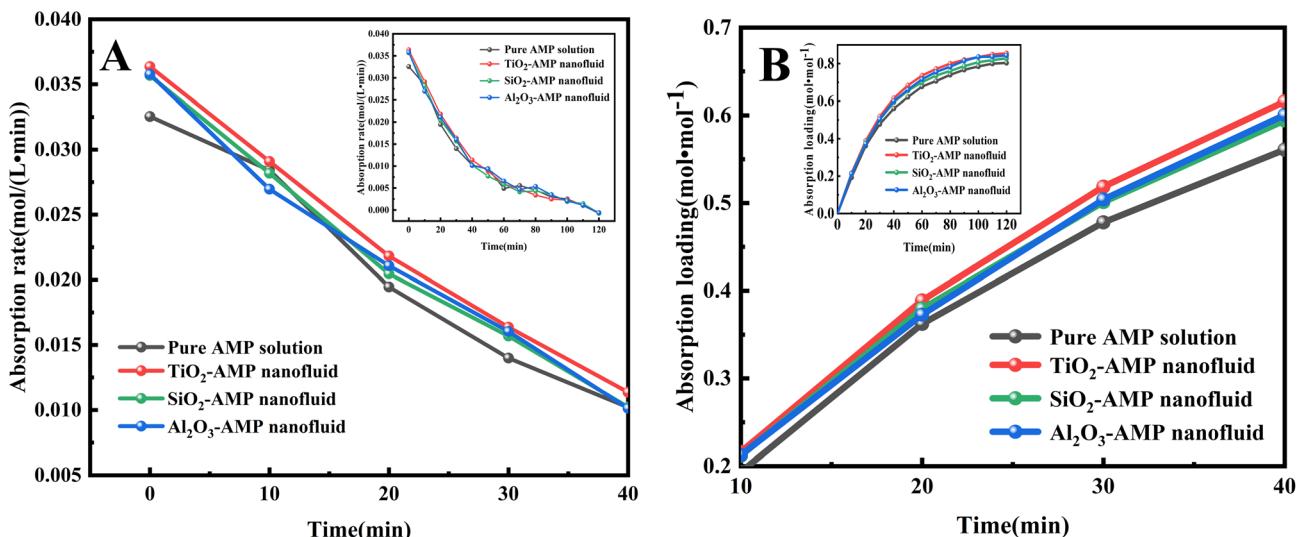
Fig. 2 (A) CO_2 absorption rate of different absorbents; (B) CO_2 absorption loading of different absorbents.
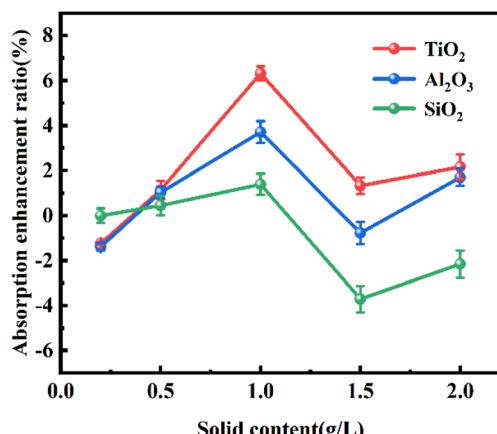

Fig. 3 Enhancement ratio of CO_2 absorption for different types of absorbents with different solid contents.

resulting in enhanced Brownian motion and increased mass transfer rate. However, when the solid content exceeds a certain value, the area of the gas–liquid interface is limited,[24] which may also increase particle agglomeration and precipitation, thereby hindering the mass transfer and leading to lower absorption loading.

3.1.3 Effect of gas flow rate. Gas volume flow rate was also found to significantly affect CO_2 absorption.[25] Herein, we investigate the effect of gas–liquid flow rate on CO_2 absorption loading by varying the CO_2 volumetric flow rate in TiO_2-AMP nanofluid (0.06/0.12/0.24/0.36 L min^{-1}). The results showed that the CO_2 absorption rate increased with increasing CO_2 volume flow rate (Fig. 4A), which was attributed to the fact that the number of bubbles entering the liquid phase and the bubble rise rate increased per unit time with increasing gas flow rate, and thus the turbulence around the bubbles was enhanced, leading to enhanced mass transfer based on the boundary mixing effect, and ultimately leading to a larger

change in the CO_2 absorption rate. In addition, it was also found that when the volume flow rate of CO_2 was 0.36 L min^{-1}, the gas flow rate was too fast, the gas–liquid contact time was shorter, and the reaction could not be carried out sufficiently, leading to an insignificant change in the absorption rate.

Moreover, different CO_2 volume fraction of 6%, 10% and 12% (Fig. 4B) was chosen to investigate the effect of initial CO_2 volume fractions on the absorption performance (Fig. 4B), and the variation of CO_2 absorption enhancement factor of TiO_2-AMP nanofluid with nanoparticle solid content was investigated as well. The enhancement factor was found to increase with the increase in initial CO_2 volume fraction when the optimum solid content was reached. According to Henry's law, it is known that as the initial CO_2 volume fraction (CO_2 partial pressure) increases, it will cause the CO_2 equilibrium concentration to increase, leading to an increase in the depth of CO_2 diffusion into the liquid phase, *i.e.*, the mass transfer depth.[22,26] In this case, more nanoparticles will enter the mass transfer boundary layer, which increases turbulence and promotes the mixing of nanofluids with different concentrations of CO_2.

3.1.4 Variation of solubility with temperature. There are also differences in CO_2 solubility at different temperatures, as shown in Fig. 5. It was possible to achieve high CO_2 loading in TiO_2-AMP nanofluids at 0.3–0.45 mol CO_2 per mol even at relatively low partial pressure of CO_2 (10–20 kPa). At a high temperature of 70–80 °C, the solubility of CO_2 decreased significantly. When the partial pressure of CO_2 was 10–100 kPa, nevertheless, the solubility of CO_2 in the nanofluid was very low at 80 °C, which was 0.01–0.05 mol CO_2 per mol.

3.1.5 Absorption cycle stability of TiO_2-AMP nanofluids. The cycling performance of an absorbent is an important judgement criterion to determine whether an absorbent can be used for industrial production. Fig. 6A shows the absorption loading of the absorbent in each cycle with pure AMP solution and 1 g L^{-1} TiO_2-AMP nanofluid as experimental objects. From the experimental results, it can be seen that the CO_2 absorption
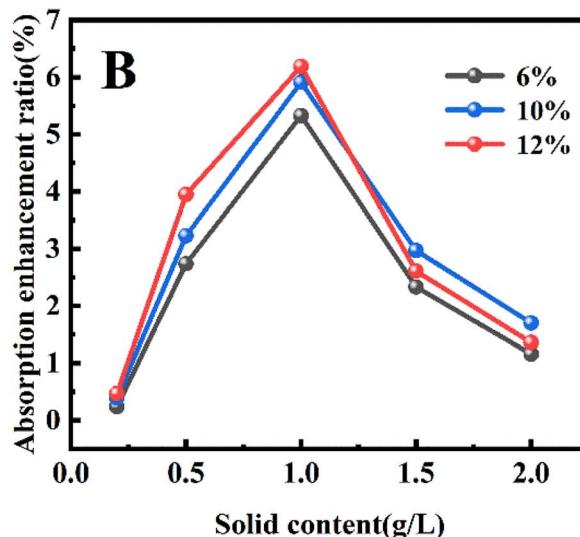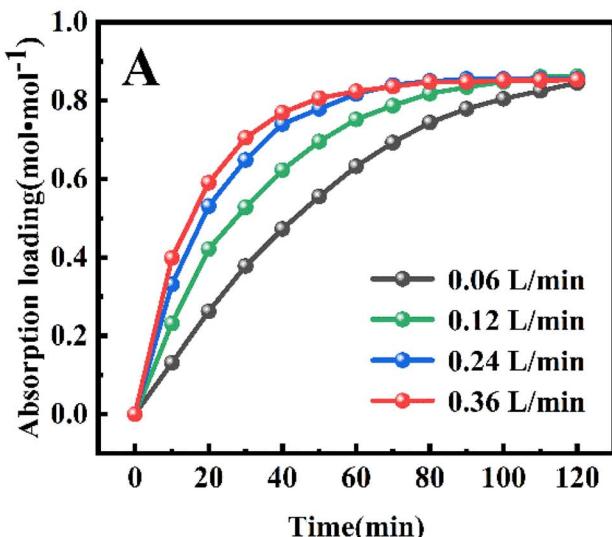
Fig. 4 (A) Effect of different CO_2 volume flow rates on CO_2 absorption loading; (B) effect of different CO_2 volume fractions on CO_2 absorption.
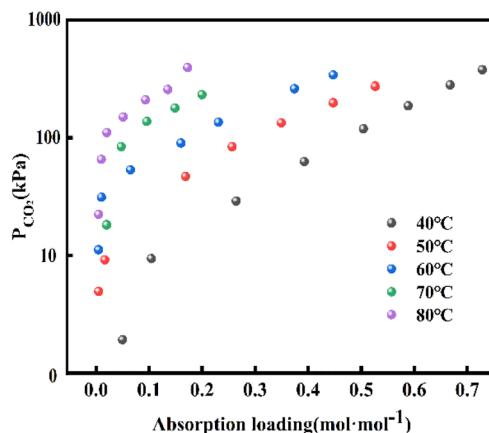

Fig. 5 Variation of CO_2 solubility with nanofluid temperature.

loading of the TiO_2-AMP nanofluid absorbent can still reach 0.6 mol CO_2 per mol amine after five cycles, which indicates that the TiO_2-AMP nanofluid has an excellent cycling performance. The CO_2 absorption loading of the nanofluid decreased by 33.33% after the 5th cycle, which is comparable to the 3rd cycle of the pure solution (Fig. 6B). This demonstrated that the incorporation of nanoparticles could improve the cycling performance of the absorbent.

3.2 Desorption performance

3.2.1 Effect of nanofluid type.
Fig. 7A represents the effect of different nanofluids on CO_2 desorption rate in the same time range. Compared with the pure AMP solution, the CO_2 desorption rate of nanofluids was much higher than the pure solution from 0 to 15 min. The TiO_2-AMP nanofluid has the largest rate of CO_2 desorption than Al_2O_3-AMP and SiO_2-AMP nanofluid, owing to the fact that there are more oxygen vacancies in TiO_2, which can adsorb more CO_2, and therefore more

CO_2 is desorbed. And at the end of the desorption process, the desorption rate can be seen to change little over time. This is because as time goes by, the CO_2 concentration inside the absorbent becomes very low and the effect of nanoparticles on the desorption performance decreases. The solid content of nanoparticles has a great influence on the rate of CO_2 desorption from the absorbent-rich liquid, as seen in Fig. 7B, the desorption rate reaches the highest at the optimal solid content of 1 g L^{-1}. Fewer nanoparticles result in less CO_2 absorption and desorption, and more nanoparticles may hinder the mass transfer. As the experimental results showed that TiO_2 nanoparticles were more effective in enhancing CO_2 desorption and the optimum solid content was 1 g L^{-1} ($\pm1.0\%$, $\pm2.5\%$).

3.2.2 Effect of desorption temperature.
As well as temperature is an important factor to influence the desorption efficiency. In this paper, the CO_2 desorption efficiency and generation cycle were investigated at different temperatures. The results in Fig. 8 clearly display that the desorption efficiency is extremely sensitive to the change of desorption temperature, whether pure AMP solution or nanofluid, and the desorption efficiency increases with the increase of desorption temperature. When the desorption temperature was increased from 80 °C to 120 °C, the desorption efficiency of the pure AMP solution increased from 86.2% to 98.3%, while the desorption efficiency of the nanofluid increased from 86% to 99%. Along with the gradual increase of temperature (especially 100 °C–120 °C), the increase of desorption efficiency becomes smaller, and the CO_2 generation cycle is shortened. The energy consumption of solvent desorption is also an important parameter,[41] and it was demonstrated by experimental results that TiO_2-AMP nanofluid can have a well desorption efficiency at a low energy consumption, where the desorption temperature is 120 °C, the desorption efficiency is high and the desorption time is shortened by 12.5%.

3.2.3 Absorption–desorption cyclic stability of different nanofluids.
To evaluate the performance of the absorbents, the
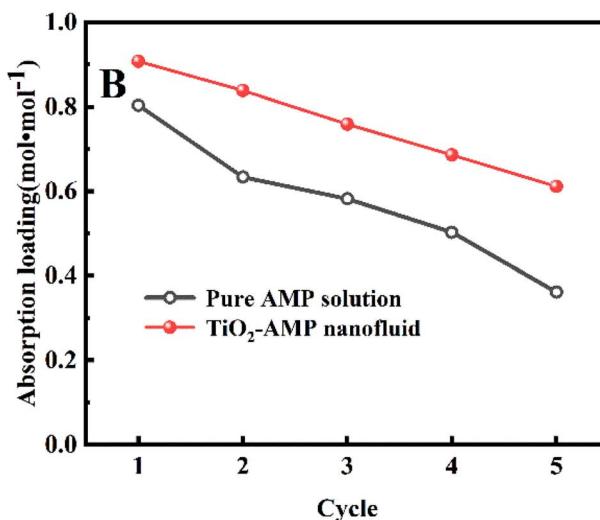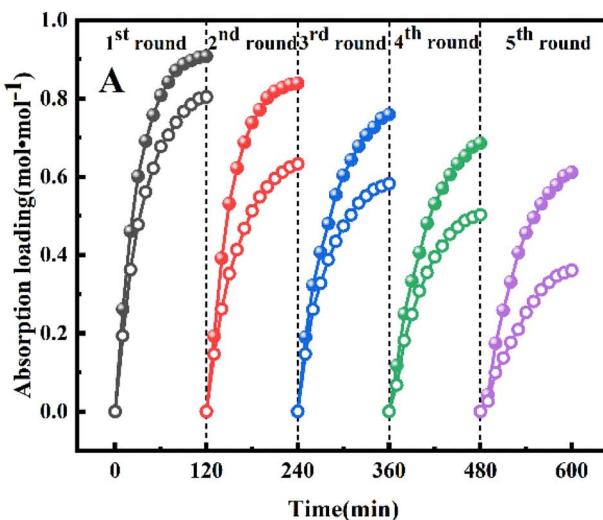
Fig. 6   (A) and (B) Comparison of the performance of nanofluid and pure solution for CO_2 multiple absorption; solid indicates TiO_2-AMP nanofluids, hollow indicates pure AMP solution.
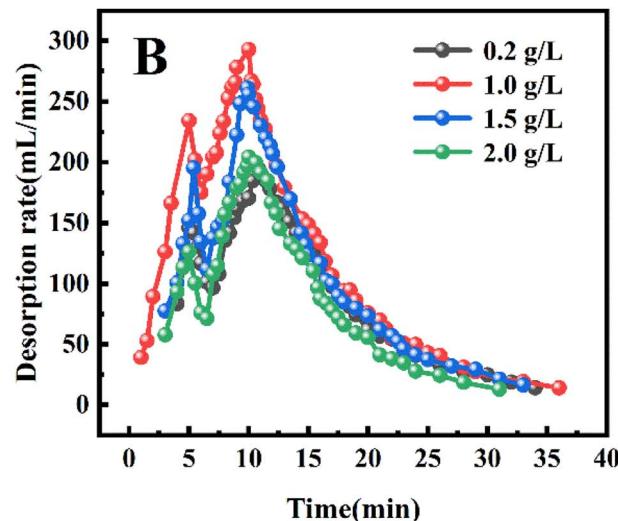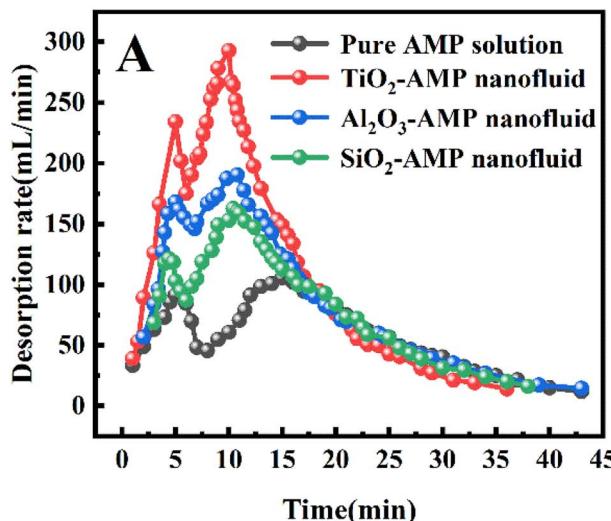

Fig. 7   (A) CO_2 desorption rates of different absorbents; (B) CO_2 desorption rates of nanofluids with different solid contents.
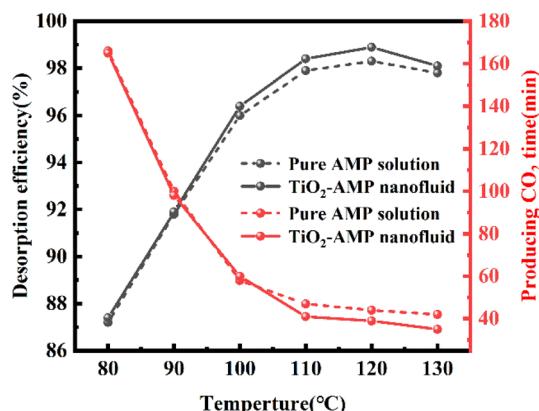

Fig. 8   Effect of desorption temperature on desorption efficiency and CO_2 generation period.

absorption–desorption cycling experiments were repeated three times for each absorbent. From the above, a higher absorption cycling loading was found for TiO_2-AMP nanofluid than the others, and its cycling desorption performance was also revealed to be superior to the other nanofluids through further desorption experiments. Upon three cycles, the TiO_2-AMP nanofluid desorption enhancement ratio reached 9.3% (Fig. 9). As a result, it was proved that the TiO_2-AMP nanofluid behaved well in CO_2 desorption likewise. Table 1 reveals a comparison of the enhancement of CO_2 desorption rate by nanofluids[42–46] with the present experiments.

3.3   Absorption/desorption enhancement mechanisms of nanofluid absorbent

Currently, a large number of studies have discussed the mechanisms of nanoparticle-enhanced CO_2 absorption/desorption in
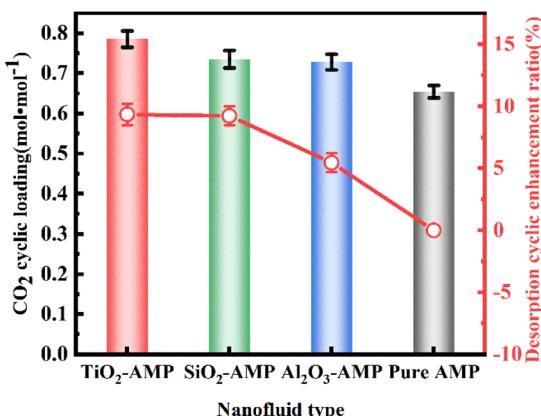
Fig. 9 Average CO_2 cyclic loading and desorption cyclic enhancement ratio for different nanofluids.

alcoholic amine solutions, but these mechanisms often only explain part of the experimental phenomena,[19–21] few desorption experiments have been carried out.[42,43] In this paper, the effect of nanoparticles on the absorption/desorption of CO_2 from AMP aqueous solutions is investigated, and the enhancement mechanism is discussed in depth using TiO_2-AMP nanofluids as an example (Fig. 10).

Firstly, the agitation of the nanofluid and the movement of the nanoparticles make the bubbles constantly collide, leading to the rupture and deformation of the CO_2 bubbles dispersed in the nanofluid, so that a larger contact area is caused, thus enhancing the absorption performance.[15,27] On the other hand, TiO_2 is a nanoparticle with high CO_2 adsorption capacity, Liu[37] et al. also modulated the preferential CO_2 adsorption sites on the material surface by interfacial effects and found that CO_2 adsorption on TiO_2 surfaces with point defects (oxygen vacancies) was significantly changed. TiO_2 nanoparticles move randomly with adsorbed CO_2 in the base solution, i.e., the particles transport additional CO_2 across the gas–liquid interface via adsorption and desorption.[28–35] The presence of oxygen vacancies introduces additional adsorption sites due to the impregnation of TiO_2 nanoparticles in the AMP base solution, and together with the spatial site-blocking effect, the stability of the system is effectively controlled,[36,40] which improves the performance of the absorbent. In terms of Al_2O_3/SiO_2-AMP nanofluids, SiO_2 nanoparticles have fewer defect sites.[38,39] Even though Al_2O_3/SiO_2 nanoparticles may hinder the gas–liquid mass transfer, their enhancement factor is less than 1. As the solid content increases, the number of nanoparticles and mutual interference increase, the nanoparticles around the bubbles prevented the bubbles from agglomerating, leading to an increase in the gas–liquid mass transfer area. Hence all these mechanisms do not act individually, but together contribute to the improvement of the absorption performance.

Further experimental results were also analyzed to determine which effect had the largest impact on enhancing CO_2 desorption. As mentioned earlier, the superior absorption properties of TiO_2-AMP nanofluids have benefited from the presence of oxygen vacancies, and the CO_2 adsorption/desorption by oxygen vacancies on the TiO_2 surface is currently more studied. It has been reported that the presence of oxygen vacancies increases the peaks of thermal desorption spectra (TDS) of TiO_2 surface at 166 K and 200 K.[47] The Brownian motion becomes more active with the increase of temperature, accelerating the desorption process. Besides, AMP's unique spatial site resistance effect makes the particles stably and uniformly distributed in the base liquid, which effectively prevents the flocculation and agglomeration of TiO_2 nanoparticles. Meanwhile, TiO_2 nanoparticles have high thermal stability, and the presence of the nanoparticles also leads to a rapid increase in the temperature of the absorbent, which allows CO_2 to be desorbed quickly. Numerous studies have confirmed the enhanced heat transfer in nanofluids.[45] As for the existence of Al_2O_3 nanoparticles, the desorption performance is reduced compared to TiO_2-AMP nanofluid, because of the high surface potential of the Al_2O_3 nanoparticles as pH varies, which also means that the desorption temperature must be applied at a much higher temperature than the traditional conditions,[48] so that CO_2 gas can be desorbed from the Al_2O_3 nanoparticles. Nevertheless, this effect does not exist in the case of semiconductor oxides (SiO_2).[43]

In general, AMP are often used as absorption enhancers and viscosity modifiers, and nanofluids are employed to capture CO_2 for lower energy consumption. In this study, it was found that the performance of nanofluids in both absorption and desorption was improved compared the pure solution. General improvement in the efficiency of the absorption–desorption system was achieved through the use of nanofluids, and it is expected that the mixed amine CO_2 capture system will be incorporated with the nanofluids mentioned in this paper to achieve a favorable absorption–desorption performance of the

Table 1 Comparison of CO_2 desorption performance of nanofluids

| Authors	Nanoparticle	Solvent	Conclusion
Wang et al.[44]	Al_2O_3 (0.1 wt%) SiO_2 (0.1 wt%)	MEA/MDEA/PZ	Enhancement performance is: PZ > MEA > MDEA
Lee et al.[46]	Al_2O_3 (0.01 vol%) SiO_2 (0.01 vol%)	DI water	Maximum CO_2 absorption/regeneration performance enhancements are 23.5% and 11.8%
Kim et al.[27]	Al_2O_3 (0.1 wt%)	Methanol	Enhanced up to 26% at 0.01 vol% compared with pure methanol
Present experiments	TiO_2 (1 g L^{-1}) Al_2O_3 (1 g L^{-1}) SiO_2 (1 g L^{-1})	AMP	Enhancement performance is: TiO_2 > SiO_2 > Al_2O_3
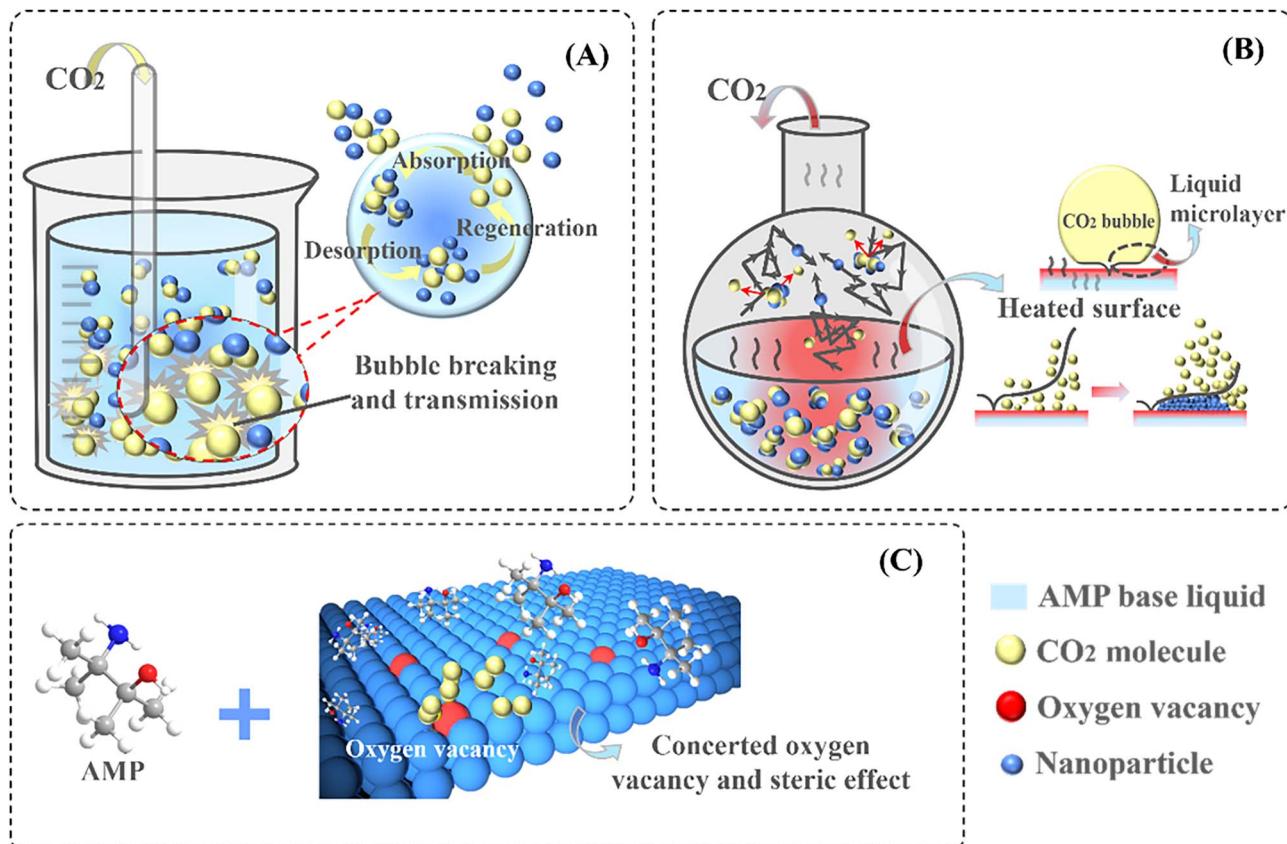
Fig. 10 (A) Absorption/(B) desorption mechanisms of TiO_2-AMP nanofluids and (C) present experiments.

CO_2 cycle. Considering the comprehensive application of the actual system, future research should be based on the actual operation and the economic benefits should also be taken into account in detail in the life cycle cost analysis, which will be carried out in the next step of this study.

4 Conclusion

In this paper, the effects of different nanoparticles on the CO_2 absorption–desorption performance of AMP-based fluids were investigated. TiO_2-AMP nanofluid, Al_2O_3-AMP nanofluid, and SiO_2-AMP nanofluid were used as absorbents and their CO_2 absorption–desorption performances were evaluated, and the following conclusions were obtained:

(1) At a certain molar concentration of base solution AMP, the CO_2 absorption rate of nanofluid were greater than pure AMP solution for the first 40 min of absorption, which indicated that nanoparticles could enhance the CO_2 absorption rate in the diffusion control phase.

(2) The CO_2 absorption capacity of TiO_2 nanoparticles was found to be better than Al_2O_3 and SiO_2 nanoparticles, and the enhancement of absorption was $TiO_2 > Al_2O_3 > SiO_2$ in descending order. The desorption enhancement factor of TiO_2 nanoparticles was also found to be higher than the others, and the enhancement of desorption was found to be $TiO_2 > SiO_2 > Al_2O_3$, and all of them exist with the optimal solid content of 1 g L^{-1} ($\pm 1.0\%$, $\pm 2.5\%$).

(3) The TiO_2-AMP nanofluid desorption enhancement ratio reached 9.2%, approximating the SiO_2-AMP nanofluid enhancement ratio.

(4) Based on the mechanism of nanofluids to promote mass transfer, combined with the unique spatial site resistance effect of AMP, the mechanisms of various nanofluids to enhance the CO_2 absorption–desorption performance were discussed.

Author contributions

Qiuli Zhang: revision, supervision, funding acquisition. Zhongyi Ning: research, experimental conducting, discussion, writing – original draft. Xuelian Li: discussion, supervision. Xiaogang Ning, Fan Wu: experimental conducting. Jun Zhou: revision, supervision.

Conflicts of interest

All co-authors have seen and agree with the contents of the manuscript and there is no financial interest to report. We certify that the submission is original work and is not under review at any other publication.

no. 2020TD-028), the Natural Science Basic Research Program of Shaanxi (Program no. 2019JLP-17).

References

1 IEA, *Global energy & CO₂ status report 2021*, International Energy Agency, 2021. https://www.iea.org/reports/global-energy-review-2021.

2 K. Zickfeld, D. Azevedo, S. Mathesius and H. D. Matthews, Asymmetry in the climate carbon cycle response to positive and negative CO₂ emissions, *Nat. Clim. Change*, 2021, **11**, 613–617, DOI: 10.1038/s41558-021-01061-2.

3 X. Zhu, H. Lu, K. Wu, Y. Zhu, Y. Liu, C. Liu and B. Liang, DBU-glycerol solution: a CO₂ absorbent with high desorption ratio and low regeneration energy, *Environ. Sci. Technol.*, 2020, **54**, 7570–7578, DOI: 10.1021/acs.est.0c01332.

4 Y. Shen, H. Chen, J. Wang, S. Zhang, C. Jiang, J. Ye, L. Wang and J. Chen, Two-stage interaction performance of CO₂ absorption into biphasic solvents: mechanism analysis, quantum calculation and energy consumption, *Appl. Energy*, 2020, **260**, 114343.

5 X. Zhou, G. Jing, B. Lv, F. Liu and Z. Zhou, Low-viscosity and efficient regeneration of carbon dioxide capture using a biphasic solvent regulated by 2-amino-2-methyl-1-propanol, *Appl. Energy*, 2019, **235**, 379–390.

6 S. K. Wai, C. Nwaoha, C. Sai wan, R. Idem and T. Supap, Absorption heat, solubility, absorption and desorption rates, cyclic capacity, heat duty, and absorption kinetic modeling of AMP−DETA blend for post-combustion CO₂ capture, *Sep. Purif. Technol.*, 2018, **194**, 89–95.

7 S.-J. Han and J.-H. Wee, CO₂ Absorption Performance and Electrical Properties of 2-Amino-2-methyl-1-propanol Compared to Monoethanolamine Solutions as Primary Amine-Based Absorbents, *Energy Fuels*, 2021, **35**(4), 3197–3207.

8 C. Nwaoha, C. Saiwan, T. Supap, R. Idem, P. Tontiwachwuthikul, W. Rongwong, M. J. Al-Marri and A. Benamor, Carbon dioxide (CO₂) capture performance of aqueous tri-solvent blends containing 2-amino-2-methyl-1-propanol (AMP) and methyl diethanolamine (MDEA) promoted by diethylenetriamine (DETA), *Int. J. Greenhouse Gas Control*, 2016, **53**, 292–304.

9 W. Conway, S. Bruggink, Y. Beyad, W. Luo, I. Melian-Cabrera, G. Puxty and P. Feron, CO₂ absorption into aqueous amine blended solutions containing mono ethanol amine (MEA), N, N-dimethylethanolamine (DMEA), N, N-diethylethanolamine (DEEA) and 2-amino-2-methyl-1-propanol (AMP) for post-combustion capture processes, *Chem. Eng. Sci.*, 2015, **126**, 446–454.

10 W. M. Budzianowski, Explorative analysis of advanced solvent processes for energy efficient carbon dioxide capture by gas-liquid absorption, *Int. J. Greenhouse Gas Control*, 2016, **49**, 108–120.

11 M. Arshadi, H. Taghvaei, M. Abdolmaleki, *et al.*, Carbon dioxide absorption in water/nanofluid by a symmetric amine-based nano-dendritic adsorbent, *Appl. Energy*, 2019, **242**, 1562–1572.

12 D. S. Mannel, G. Qi, L. R. Widger, *et al.*, Enhancements in mass transfer for carbon capture solvent part II: Micron-sized solid particles, *Int. J. Greenhouse Gas Control*, 2017, **61**, 138–145.

13 P. Agarwal, H. Qi and L. A. Archer, The ages in a self-suspended nanoparticle liquid, *Nano Lett.*, 2010, **10**(1), 111–115.

14 Z. Zhang, J. Cai, F. Chen, *et al.*, Progress in enhancement of CO₂ absorption by nanofluids: A mini review of mechanisms and current status, *Renewable Energy*, 2018, **118**, 527–535.

15 W. G. Kim, H. U. Kang, K. M. Jung and S. H. Kim, Synthesis of silica nanofluid and application to CO₂ absorption, *Sep. Sci. Technol.*, 2008, **43**(11e12), 3036e55.

16 J. K. Lee, J. Koo, H. Hong and Y. T. Kang, The effects of nanoparticles on absorption heat and mass transfer performance in NH₃/H₂O binary nanofluids, *Int. J. Refrig.*, 2010, **33**(2), 269e75.

17 X. Ma, F. Su, J. Chen, T. Bai and Z. Han, Enhancement of bubble absorption process using a CNTs-ammonia binary nanofluid, *Int. Commun. Heat Mass Transfer*, 2009, **36**, 657e60.

18 H. Kim, J. Jeong and Y. T. Kang, Heat and mass transfer enhancement for falling film absorption process by SiO₂ binary nanofluids, *Int. J. Refrig.*, 2012, **35**(3), 645e51.

19 W. Yu, T. Wang, A.-H. A. Park, *et al.*, Review of liquid nano-absorbents for enhanced CO₂ capture, *Nanoscale*, 2019, **11**(37), 17137–17156.

20 J. Zhang, S. Li, L. Peng, *et al.*, Progress in research on gas-liquid mass transfer enhancement of nanofluids, *Chem. Ind. Eng. Prog.*, 2013, **32**(4), 732–739.

21 S. Y. Cheng, Y. Z. Liu and G. S. Qi, Progress in the enhancement of gas-liquid mass transfer by porous nanoparticle nanofluids, *J. Mater. Sci.*, 2019, **54**(20), 13029–13044.

22 A. N. Turanov and Y. V. Tolmachev, Heat- and mass-transport in aqueous silica nanofluids, *Heat Mass Transfer*, 2009, **45**, 1583–1588.

23 N. Keshishian, M. Nasr Esfahany and N. Etesami, Experimental investigation of mass transfer of active ions in silica nanofluids, *Int. Commun. Heat Mass Transfer*, 2013, **46**, 148–153.

24 S. Karve and V. A. Juvekar, Gas absorption into slurries containing fine catalyst particles, *Chem. Eng. Sci.*, 1990, **45**, 587–594.

25 J. Z. Jiang, B. Zhao, Y. Q. Zhuo, *et al.*, Experimental study of CO₂ absorption in aqueous MEA and MDEA solutions enhanced by nanoparticles, *Int. J. Greenhouse Gas Control*, 2014, 29135–29141.

26 Y. M. Xuan and Q. Li, *Nanofluid Energy Transfer Theory and Application*, Science Press, Beijing, 2010, pp. 154–162.

27 J. H. Kim, C. W. Jung and Y. T. Kang, Mass transfer enhancement during CO₂ absorption process in methanol/Al₂O₃ nanofluids, *Int. J. Heat Mass Transfer*, 2014, **76**, 484–491.

28 L. J. Won, P. I. Torres, L. J. Hun., *et al.*, Combined CO₂ absorption/regeneration performance enhancement by

using nano-absorbents, *Applied energy*, 2016, **178**(Sep.15), 164–176.

29 E. Alper, B. Wichtendahl and W. D. Deckwer, Gas-absorption mechanism in catalytic slurry reactors, *Chem. Eng. Sci.*, 1980, **35**, 217–222.

30 E. Alper and S. Ozturk, The effect of activated carbon loading on oxygen absorption into aqueous sodium sulfide solutions in a slurry reactor, *Chem. Eng. J. Biochem. Eng. J.*, 1986, **32**, 127–130.

31 J. T. Tinge and A. A. H. Drinkenburg, Absorption of gases into activated carbon water slurries in a stirred cell, *Chem. Eng. Sci.*, 1992, **47**, 1337–1345.

32 J. H. J. Kluytmans, B. G. M. van Wachem, B. F. M. Kuster and J. C. Schouten, Mass transfer in sparged and stirred reactors: influence of carbon particles and electrolyte, *Chem. Eng. Sci.*, 2003, **58**, 4719–4728.

33 V. Linek, M. Kordac and M. Soni, Mechanism of gas absorption enhancement in presence of fine solid particles in mechanically agitated gas–liquid dispersion. Effect of molecular diffusivity, *Chem. Eng. Sci.*, 2008, **63**, 5120–5128.

34 S. Kim, R. Xu, W. Lee, C. K. Choi and Y. T. Kang, CO_2 absorption performance enhancement by dodecane nano emulsion absorbents, *J. CO2 Util.*, 2019, **30**, 18–27.

35 J. A. Eastman, S. U. S. Choi, S. Li, *et al.*, Anomalously increased effective thermal conductivities of ethylene glycol-based nanofluids containing copper nanoparticles, *Appl. Phys. Lett.*, 2001, **78**(6), 718–720.

36 Z. Sheng nan, T. Lina, Y. Lixin, *et al.*, Phosphine-based ionic liquids for CO_2 chemical fixation: Improving stability and activity by asymmetric flexible steric hindrance, *J. Environ. Chem. Eng.*, 2023, **11**(3), 109883.

37 L. Liu, Z. Liu, H. Sun, *et al.*, Morphological effects of Au[13] clusters on the adsorption of CO_2 over anatase TiO_2 (101), *Appl. Surf. Sci.*, 2017, **399**, 469–479.

38 G. Pragati, J. G. Navea, S. C. Larsen, *et al.*, Carbon dioxide (C~ (16)O_22 and C~ (18)O_2) adsorption in zeolite Y materials: effect of cation, adsorbed water and particle size, *Energy Environ. Sci.*, 2009, **2**(4), 401–409.

39 A. Haghtalab, M. Mohammadi and Z. Fakhroueian, Absorption and solubility measurement of CO2 in water-based ZnO and SiO2 nanofluids, *Fluid Phase Equilib.*, 2015, **392**, 33–42.

40 T. L. Thompson, O. Diwald, J. Yates, *et al.*, CO_2 as a Probe for Monitoring the Surface Defects on TiO_2 (110) Temperature-Programmed Desorption, *J. Phys. Chem. B*, 2003, **107**(42), 11700–11704.

41 P. Zhang, Y. Shi and J. Wei, Regeneration of 2-amino-2-methyl-1-propanol used for carbon dioxide absorption, *J. Environ. Sci.*, 2008, **20**(1), 39–44.

42 J. W. Lee, I. T. Pineda, J. H. Lee and Y. T. Kang, Combined CO_2 absorption/regeneration performance enhancement by using nano-absorbents, *Appl. Energy*, 2018, **178**, 164–176.

43 J. S. Lee, J. W. Lee and Y. T. Kang, CO_2 absorption/regeneration enhancement in DI water with suspended nanoparticles for energy conversion application, Appl, *Energy*, 2015, **143**, 119–129.

44 T. Wang, W. Yu, F. Liu, M. Fang, M. Farooq and Z. Luo, Enhanced CO_2 absorption and desorption by mono ethanolamine (MEA)-based nanoparticle suspensions, *Ind. Eng. Chem. Res.*, 2016, **55**(28), 7830–7838.

45 X. Jiajun, Y. Bao and H. Boualem, Thermophysical Properties and Pool Boiling Characteristics of Water-in-Polyalphaolefin Nanoemulsion Fluids, *J. Heat Transfer*, 2013, **135**(9), 0913031–0913036.

46 J. H. Lee, J. W. Lee and Y. T. Kang, CO_2 regeneration performance enhancement by nanoabsorbents for energy conversion application, *Appl. Therm. Eng.*, 2016, **103**, 980–988.

47 T. L. Thompson, O. Diwald, J. Yates, *et al.*, CO_2 as a Probe for Monitoring the Surface Defects on TiO_2 (110) Temperature-Programmed Desorption, *J. Phys. Chem. B*, 2003, **107**(42), 11700–11704.

48 L. J. Won, P. I. Torres, L. J. Hun., *et al.*, Combined CO_2 absorption/regeneration performance enhancement by using nanoabsorbents, *Appl. Energy*, 2016, **178**, 164–176.

49 L. Fang, H. Liu, Y. Bian, *et al.*, Experimental Study on Enhancement of Bubble Absorption of Gaseous CO_2 with Nanofluids in Ammonia, *J. Harbin Inst. Technol.*, 2017, **24**(02), 80–86.